Elevated temperature alters microbial communities, but not decomposition rates, during three years of in-situ peat decomposition

Spencer Roth[1], Natalie A. Griffiths[2,3], Randall K. Kolka[4], Keith C. Oleheiser[2,3], Alyssa A. Carrell[1], Dawn M. Klingeman[1], Angela Seibert[5], Jeffrey P. Chanton[6], Paul J. Hanson[2,3], and Christopher W. Schadt[1,3,7,*]

[1]Biosciences Division, Oak Ridge National Laboratory, Oak Ridge, TN, USA 37830

[2]Environmental Sciences Division, Oak Ridge National Laboratory, Oak Ridge, TN, USA 37830

[3]Climate Change Science Institute, Oak Ridge National Laboratory, Oak Ridge, TN, USA 37830

[4]Northern Research Station, USDA Forest Service, Grand Rapids, MN, USA 55744

[5]Department of Geosciences, Boise State University, Boise, ID, USA 83725

[6]Department of Earth, Ocean, and Atmospheric Science, Florida State University, Tallahassee, FL, USA 32306

[7]Department of Microbiology, University of Tennessee, Knoxville, TN, USA 37996

*Author for correspondence: Christopher Schadt, schadtcw@ornl.gov

Key words: Peatlands, climate change, microbiome, organic matter decomposition,

This manuscript has been authored by UT-Battelle, LLC under Contract No. DE-AC05-00OR22725 with the U.S. Department of Energy. The United States Government retains and the publisher, by accepting the article for publication, acknowledges that the United States Government retains a non-exclusive, paid-up, irrevocable, world-wide license to publish or reproduce the published form of this manuscript, or allow others to do so, for United States Government purposes. The Department of Energy will provide public access to these results of federally sponsored research in accordance with the DOE Public Access Plan (http://energy.gov/downloads/doe-public-access-plan).

Abstract:

Peatlands store approximately one-third of the global terrestrial carbon and are historically considered carbon sinks due to primary production outpacing microbial decomposition of organic matter. Climate change has the potential to alter the rate at which peatlands store or release carbon, and results from the Spruce and Peatland Responses Under Changing Environments (SPRUCE) experiment have shown net losses of organic matter and increased greenhouse gas production from a boreal peatland in response to whole-ecosystem warming. In this study, we utilized the SPRUCE sites to investigate how warming and elevated CO_2 impact peat microbial communities and peat soil decomposition. We deployed peat soil decomposition ladders across warming and CO_2 treatment enclosures for three years, after which we characterized bacterial, archaeal, and fungal communities through amplicon sequencing and measured peat mass and compositional changes across four depth increments. Microbial diversity and community composition were significantly impacted by soil depth, temperature, and CO_2 treatment. Bacterial/archaeal α-diversity increased significantly with increasing temperature, and fungal α-diversity was significantly lower under elevated CO_2 treatment. Trans-domain microbial networks showed higher complexity (nodes, edges, degree, betweenness centrality) of microbial communities in decomposition ladders from warmed enclosures, and the number of highly connected, hub taxa within the networks was positively correlated with temperature. Methanogenic hubs were identified in the networks constructed from the warmest enclosures, indicating increased importance of methanogenesis in response to warming. Microbial community responses were not however reflected in measures of peat soil decomposition, as warming and elevated CO_2 had no significant short-term effects on soil mass loss or composition. Regardless of treatment, on average only 4.5% of the original soil mass was

lost after three years and variation between replicates was high, potentially masking treatment effects. Many previous studies from the SPRUCE experiment have shown that warming is accelerating organic-matter decomposition and CO_2 and CH_4 production, and our results suggest that these changes may be driven by warming-induced shifts in microbial communities.

1. Introduction:

Despite covering less than 10% of the Earth's surface, peatlands contain approximately one-third of all global terrestrial organic matter (OM) [1-3]. Peatland organic soil deposits can be several meters deep, the result of thousands of years of net primary production outpacing OM mineralization. Microorganisms are primarily responsible for OM degradation in peatlands [4, 5]; however, anoxic, acidic, oligotrophic, and cold conditions that are common across northern peatlands greatly constrain microbial activity [4].

Climate change has the potential to alter peatland biogeochemistry, especially at northern latitudes where warming is occurring at an accelerated pace compared to equatorial regions [6]. The large carbon stocks in northern peatlands that have built up over millennia may therefore be vulnerable to climate change [7]; however, the effects of warming and increased atmospheric CO_2 on peatland ecosystems remain to be fully described [8, 9]. The Spruce and Peatland Responses Under Changing Environments (SPRUCE) experiment is a long-term warming and elevated CO_2 experiment investigating peatland responses to climate change on an ecosystem level (https://mnspruce.ornl.gov/). Since 2016, whole-ecosystem warming up to +9 ºC above ambient has been applied to a boreal peatland in a regression-based design. In addition, elevated air partial pressure of CO_2 has been applied to half of the 10 SPRUCE experimental enclosures.

72 Results from the SPRUCE experiment have shown significant, rapid loss of carbon from the
73 peatland with increasing temperature [10] concomitant with a large decline and death of
74 *Sphagnum sp*. at the highest temperatures, that contribute the largest share of Gross Primary
75 Production (GPP) in these ecosystems [11]. In addition, porewater concentrations of CO_2 and
76 CH_4 have been shown to correlate with temperature treatment at SPRUCE [12], and radiocarbon
77 analysis of soil suggests that warming is promoting microbial respiration of solid-phase peat
78 [13]. Similar results have also been obtained in studies of other peatlands [14-16], and in
79 incubation studies that show increasing CH_4 and CO_2 production with warming [17, 18].
80 Net losses of carbon from the SPRUCE sites have been attributed to increased degradation of
81 OM, rather than a reduction in primary production [10]. Under anoxic conditions, microbial
82 degradation of OM involves multiple steps including hydrolysis, fermentation, and anaerobic
83 respiration. Mineralization of carbon to CO_2 and CH_4 in peatlands therefore relies on microbial
84 metabolic interactions which may be altered by climate change. Incubation experiments have
85 demonstrated that microbial activities [19, 20] and metabolic interactions are significantly altered
86 by warming [15], although impacts on community structure and diversity vary [17, 18, 21, 22].
87 *In situ* results showing increasing CH_4:CO_2 with warming suggest that microbial interactions in
88 the SPRUCE sites may be altered to favor increased methanogenesis [12, 23].
89 Previous studies have investigated the effects of warming on peat soil decomposition through
90 incubations or whole-ecosystem assessments [10, 12, 13, 17, 18, 24]. Valuable insights have
91 been gained from these experiments; however, incubation studies do not fully reflect
92 environmental conditions, and "bottle effects" may influence microbial community structure
93 [25]. Conversely, assessing decomposition from *in situ* environmental measurements is complex
94 and may be influenced by other ecosystem processes such as changes in primary productivity. To

95 overcome these limitations, we utilized new peat soil decomposition ladders, which are peat litter
96 bags attached to a rigid frame, to assess the impacts of temperature, and CO_2 treatments on peat
97 soil decomposition at four depths. This approach allows for *in situ* investigation of
98 decomposition while controlling for the effects of primary productivity and excluding fresh litter
99 inputs. While studies of fresh plant litter decomposition using similar methods are quite common
100 across many forest ecosystem types[26], studies of soil and particularly peat decomposition
101 using decomposition bag methods appear to be absent from the literature. Peat decomposition
102 ladders were deployed in the top 40 cm of peat in the 10 SPRUCE experimental enclosures, as
103 changes in OM mineralization have been most pronounced in the surface and intermediate layers
104 of peat [12, 24, 27]. Following a three-years of *in situ* incubation, we measured changes in peat
105 soil mass and chemical composition and characterized microbial communities in the
106 decomposition bags through amplicon sequencing and network analyses. We hypothesized that
107 decomposition of peat soil would increase with increasing temperature, driven by changes in
108 their microbial communities.
109

110 **2. Methods:**

111 *2.1 Site description*

112 The SPRUCE experiment is located on the S1 bog (low pH, acid organic soil environment) at
113 the USDA Forest Service Marcell Experimental Forest, MN, USA. The SPRUCE site
114 description, experimental design, warming, and CO_2 treatments have been previously described
115 in detail [28]. Briefly, above- and belowground, whole-ecosystem warming has been applied in a
116 regression-based design to 10 open-air enclosures on the S1 bog since August 2015. Enclosures

are duplicated for each level of warming (+0 ºC, +2.25 ºC, +4.5 ºC, +6.75 ºC and +9 ºC above ambient), and half of the enclosures receive an elevated CO_2 atmosphere (+500 ppm).

2.2 Peat ladder construction, deployment, and retrieval

Organic soil used in the decomposition ladders was collected from within the S1 bog but outside of the footprint of the SPRUCE enclosures. Soil was collected from four depths using a Macaulay peat corer (0-10, 10-20, 20-30, and 30-40 cm), brought back to the laboratory, and air dried. After air drying, soil from each depth was homogenized by breaking up the dried soil using sieves, and large fragments of vegetation (i.e., roots) were removed. Soil was then weighed (2.4-4.2 g air-dry weight, corresponding to an approximate wet weight of 20 g) and placed into fine-mesh bags (7-µm mesh size) which were then heat sealed [29, 30].

The fine-mesh bags were placed into decomposition ladders which were made of acrylonitrile butadiene styrene plastic (design from J. Patrick Megonigal, personal communication, 2016). The ladders were placed vertically in the peat profile to allow for depth-specific measurements of soil decomposition. Each ladder had four openings (6.5 cm wide by 9 cm tall) corresponding to the four soil depths (Figure S1). Each ladder was constructed by placing four, soil-filled, fine-mesh bags, one from each depth, between two plastic ladder holders. The ladders were lined with mesh (0.5 x 1.0 mm mesh size) to reduce abrasion of the fine-mesh bags during deployment and retrieval. The two ladder holders were closed with plastic fasteners.

The ladders were deployed on October 2, 2017 in the ten SPRUCE enclosures. Ladders were placed vertically into the peat so that the peat collected from 0-10 cm was incubated at that same depth. Three replicate ladders were deployed per enclosure and retrieval date. The replicate ladders were placed in three different hollow locations that are associated with companion litter

and wood decomposition studies within an enclosure. Three replicate ladders per enclosure were deployed and immediately retrieved from the peatland for measurement of initial mass and chemistry (t=0 y; T_0). On October 15, 2020 (t=3 y; T_f), three replicate ladders per enclosure were retrieved to measure soil mass loss, changes in chemistry, and microbial community composition.

2.3 Peat soil mass loss and carbon, nitrogen, and phosphorus analyses

After retrieval, ladders were placed into individual plastic bags and were stored at 4 °C until processing (within 24 hours). Next, each fine-mesh bag was carefully removed from the ladder and the soil was weighed to determine wet mass. For the T_f bags, soil from each mesh bag was sub-sampled so that ~1/2 was retained for dry mass and chemistry measurements, ~1/4 was frozen at -20 °C for microbial community analyses, and the remainder was frozen (-20 °C) for archival purposes. Soil collected at T_0 was not sub-subsampled as only dry mass and chemistry measurements were conducted.

Soil samples for mass loss and chemistry were air dried in a drying room (humidity <30%) for 1-2 months (until the change in mass was <5%) and then weighed. A subsample from each T_f sample was oven-dried to calculate an air-dry to oven-dry conversion factor and to calculate percent peat mass loss on an oven-dry basis. Peat used in construction of decomposition bags were not oven-dried prior to installation (T_0) into the enclosures to prevent changes in organic matter quality, however, initial masses were corrected based on the air-dry to oven-dry conversion calculated from each sample at T_f. Each air-dried sample from T_0 and T_f was ground (IKA Tube Mill grinder, Wilmington, NC, USA) and a subsample was analyzed for

162 carbon and nitrogen content using a combustion elemental analyzer (LECO-CHN628 analyzer,
163 St. Joseph, MI, USA).

164 *2.4 FTIR analysis*

165 Fourier Transform Infrared Spectroscopy (FTIR) analysis was performed on the peat
166 ladders to analyze the response of peat soil organic carbon fractions to enclosure treatments. The
167 peat soil was ground into a homogenous powder using a Spex Sampleprep 5100 mixer-mill.
168 FTIR spectra were collected using a JASCO 6800 FT-IR Spectrometer. Approximately 0.003 g
169 of sample powder was secured onto the quartz crystal (Si/CaF2), and infrared light from
170 wavenumbers 4000 cm^{-1} – 650 cm^{-1} was transmitted onto the sample at a resolution of 4 cm^{-1}.
171 Each spectrum was attenuated total reflection corrected and baseline corrected to account for
172 variability in the beam penetration depth. To produce the functional data for molecular
173 composition analysis, eight spectra per sample were averaged.

174 The spectra data were analyzed using Hodgkins' normalization method [31]. Instrument
175 and matrix variation impact on sample spectra absorbance were accounted for by dividing the
176 baseline-corrected peak heights by the total integrated area of the spectrum. Using the maximum
177 baseline-corrected absorbance between peak endpoints, the aromatics and carbohydrates
178 functional group locations were identified. The normalized aromatics spectral peak heights were
179 located at 1510 cm^{-1} and 1615 cm^{-1}. The normalized carbohydrate spectral peak height was at
180 1040 cm^{-1}. Each of these peak heights was used to calculate the percent of aromatics and
181 carbohydrates in each sample.

182 *2.5 DNA extraction and sequencing*

183 DNA was extracted from ~0.2 g of field-wet peat soil from all samples using the Qiagen
184 DNeasy 96 PowerSoil Pro QIAcube HT Kit (Qiagen, Venlo, The Netherlands) following the

185 manufacturer's protocol. Amplicon metagenomic sequencing libraries were prepared as
186 described in the Illumina 16S metagenomic sequencing library preparation guide (Part 15044223
187 Rev B) with a mixture of 515F and 806R primers for archaea/bacteria and custom primers
188 designed to the ITS2 gene region for fungi [32, 33]. Pooled libraries for each sample type were
189 validated on an Agilent Bioanalyzer (Agilent, Santa Clara, CA) using a DNA7500 chip, and the
190 final library pool concentration was determined on an Invitrogen Qubit (Waltham, MA) with the
191 broad range double stranded DNA assay. Paired end sequencing (2x 251x 8x 8) was competed
192 on an Illumina MiSeq instrument (Illumina, San Diego, CA) using v2 chemistry. Due to low base
193 diversity of the amplicons, PhiX control DNA was included in the sequencing run.

194 *2.6 Sequence analysis*

195 Demultiplexed 16S rRNA (V4 region) and ITS2 paired-end sequences were imported into
196 QIIME2 (v. 2021.4) [34]. ITS2 primer sequences were removed using the *cutadapt* plugin [35],
197 and all sequencing runs were individually denoised using the dada2 plugin [36]. Resulting
198 feature tables and representative sequences were merged for downstream analyses. Taxonomy
199 was assigned using the silva database (16S) [37] and UNITE database (ITS) [38]. Sequences and
200 feature tables were filtered based on taxonomic assignments to include only Bacteria and
201 Archaea, removing Chloroplast and Mitochondria sequences (16S) and Fungi with taxonomy
202 assigned to the phylum level at minimum (ITS). A rooted phylogenetic tree was built for each
203 dataset using the *align-mafft-to-fasttree* pipeline [39] in the *phylogeny* plugin.

204 *2.7 Statistical analyses*

205 All statistical analyses and figures were produced in R v. 4.1.0 with the *vegan* [40], *car*,
206 *phyloseq* [41], *ggplot2* [42], *microbiome*, *SpeicEasi* [43], *igraph* [44], and *hilldiv* [45] packages.
207 ITS and 16S feature tables, taxonomy, rooted phylogeny, and associated metadata were imported

208 and analyzed as *phyloseq* objects. Based on the regression design of SPRUCE, temperature
209 treatment (+0 ºC, +2.25 ºC, +4.5 ºC, +6.75 ºC, +9 ºC) was used as a continuous variable for all
210 statistical analyses. Soil depth and CO_2 treatment were treated as categorical variables, and
211 depth-specific subsets of the data were generated to investigate the effects of temperature and
212 CO_2 at a given depth. Samples were rarefied for α-diversity analyses (16S rarefaction depth =
213 9500; ITS rarefaction depth = 1000). The *hilldiv* package was used to calculate α-diversity
214 metrics as Hill numbers (effective number of species) [46], and two-way ANOVA analysis was
215 used to investigate the effects of temperature, soil depth, CO_2 treatment, and the interaction
216 between temperature and depth on α-diversity. Bray-Curtis dissimilarities [47] of total sum
217 scaled data were calculated and used to assess the effects of temperature, depth, CO_2 treatment,
218 and the interaction between temperature, CO_2, and soil depth on community composition by
219 PERMANOVA. Principal coordinates analysis plots of Bray-Curtis dissimilarities were
220 generated to visualize community composition. The *betadisper* function was used to assess
221 differences in β-dispersion across depths, temperature treatments, and CO_2 treatments.
222 Trans-domain networks were generated using the *SpiecEasi* and *iGraph* packages in R.
223 Networks were constructed for each temperature treatment and included all depths within a given
224 temperature treatment (n=24 network^{-1}). Phyloseq objects were filtered by temperature treatment,
225 and only amplicon sequence variants (ASVs) with a total sum of > 5 (16S) or > 3 (ITS) and an
226 occurrence in > 20% of the samples were included in the network analyses. If a sample was
227 lacking either a 16S or ITS library after filtering, the sample was excluded from analysis.
228 Networks parameters were set as method=mb, nlambda=50, lambda.min.ratio=1e-3, and
229 thresh=0.01. Empty nodes were removed, and networks were visualized using *phyloseq*. The
230 number of nodes, edges, node degree and betweenness centrality were calculated for each

network with the *igraph* package. Network hubs were identified by selecting nodes that had degree and betweenness centrality measures in the 90th percentile, indicating high connectedness and centrality in the network. Pearson correlation was used to investigate the relationship between network topology and SPRUCE temperature treatments.

Kruskal-Wallis test was used to compare peat soil mass and composition at T_0 to T_f. Effect sizes for T_0-T_f comparisons were calculated as $(\chi^2 - 1)/(n - 2)$, where χ^2 is the Kruskal-Wallis test result and n is the number of samples. Linear models were used to assess the effect of depth, temperature treatment, and CO_2 treatment on soil mass loss and compositional changes.

2.8 Data availability

Amplicon sequences generated in this study have been deposited in the NCBI SRA under BioProject ID PRJNA941900. All code used in statistical analysis of the data and generation of figures is available at https://github.com/swroth/Peat_Decomp_SPRUCE.

3. Results:

3.1 Community summary

Bacterial/archaeal communities were dominated by the phylum *Acidobacteriota* across soil depths and temperature treatments (28-46% mean relative abundance) (Figure S2). Near the surface (0-10 cm and 10-20 cm), *Actinobacteriota*, *Proteobacteria*, and *Planctomycetota* comprised approximately 35-45% of the bacterial/archaeal communities, while accounting for < 20% of the total community at 20-30 cm and 30-40 cm (Figure S2). Dominant phyla of the fungal communities also varied across depth, with *Basidiomycota* in highest relative abundance at 0-10 cm (~62% average relative abundance), and *Ascomycota* dominating in the deeper three depths (~54-68% average relative abundance) (Figure S3).

3.2 Microbial community composition and α-diversity are significantly influenced by temperature and CO_2 treatments

Bacterial/Archaeal and fungal community compositions were significantly impacted by depth, temperature treatment, CO_2 treatment, and the interactive effects of these variables (Figure 1, Table 1). Of the variables investigated, depth was the most influential factor driving compositional differences in the bacterial/archaeal and fungal communities, explaining 25% and 11% of the variation, respectively (Table 1). Temperature treatment explained 6.1% of the variation in the bacterial/archaeal community and 4.9% in the fungal community, and CO_2 treatment accounted for 1.9% and 2.7% of the variation for both bacterial/archaeal and fungal communities respectively (Table 1). Significant interactive effects between soil depth and temperature treatment, and between temperature treatment and CO_2 treatment were observed for the bacterial/archaeal communities (Table 1). Significant interactions between all tested variables were observed for fungal communities, such that temperature and CO_2 treatment only influenced fungal community composition at specific depths (Table 1). No significant differences in β-dispersion were observed across soil depth, temperature treatment, or CO_2 treatment.

Bacterial/archaeal α-diversity was significantly highest near the surface and declined with depth across all levels of q (species richness at q=0, Shannon entropy at q=1, Inverse Simpson at q=2) (Figure 2A, Figure S4, Table 2). Temperature treatment also significantly impacted α-diversity, with highest diversity measured in decomposition ladders from the +9 ºC enclosures across all α-diversity metrics (Figure 2A, Figure S4, Table 2). Bacterial/archaeal α-diversity was significantly higher in elevated CO_2 enclosures when compared to ambient CO_2 at q=0 and q=1 (Figure 2A, Figure S4A, Table 2). At q=2, no effect of CO_2 on α-diversity was observed, suggesting that CO_2 treatment has a limited effect on abundant bacterial/archaeal taxa (Figure

277 S4B, Table 2). In contrast, fungal α-diversity was significantly lower in enclosures with elevated
278 CO_2 when compared to ambient CO_2 enclosures across all α-diversity metrics measured (Figure
279 2B, Figure S5, Table 2). Soil depth only significantly impacted fungal species richness (q=0),
280 with highest richness observed at 0-10 cm, and we observed a significant effect of temperature
281 treatment at q=2 (Figure 2B, Figure S5, Table 2) and significant interactive effects of
282 temperature and depth at q=1 and q=2, such that temperature effects on fungal α-diversity were
283 depth specific.

284 *3.3 Trans-Domain networks*

285 We constructed temperature treatment-specific, trans-domain networks to investigate the
286 impact of temperature treatment on the connectedness of microbial communities through
287 comparisons of network topology (Figure S6). The microbial network from +0 ºC enclosures
288 across all depths had the lowest number of nodes (taxa), edges (connections between taxa), and
289 average degree (mean number of edges per node), collectively indicating lower complexity of the
290 microbial communities in +0 ºC enclosures when compared to warmed enclosures (Figure 3).
291 The number of nodes and edges and the average degree peaked in the network built from +4.5 ºC
292 enclosures (Figure 3A,B,C). Networks built from all the temperature treatments included
293 bacterial, archaeal, and fungal nodes, with the highest number of archaeal nodes present in the +9
294 ºC network (35 nodes), and the most fungal nodes occurring in the +4.5 ºC network (126 nodes)
295 (Figure 3B).

296 Within each temperature treatment network, we identified hub taxa as those with degree and
297 betweenness centrality measures in the 90th percentile. The number of hub taxa was significantly
298 correlated with temperature ($R^2 = 0.975$, $p = 0.005$), with a high of 71 hubs in the +9 ºC network
299 (Figure 3D). Archaeal hubs were present in the +4.5 ºC, +6.75 ºC and +9 ºC networks, and

300 fungal hubs were observed in all networks except the +2.25 ºC network (Figure 3D). Class-level
301 taxonomic distribution of the hub taxa revealed that *Acidobacteriae* were the most prominent
302 across all treatments and depths, followed by the *Verrucomicrobiae* (Figure 4). In the +9 ºC
303 network, six unique classes were represented in the hubs, including the methanogenic class
304 *Methanosarcinia* (Figure 4). Two unique classes were present in the +0 ºC network hubs,
305 *Myxococcia* and *Dehalococcoidia* (Figure 4). Only three of the fungal hubs could be assigned to
306 a guild by FUNguild analysis, including possible ectomycorrhizal and saprotrophic
307 *Agaricomycetes* hubs and a *Sordariomycetes* hub that is a probable plant pathogen.

308 *3.4 Peat soil mass loss and compositional changes are highly variable*

309 On average, the mass of peat soil in decomposition ladders was significantly lower after three
310 years of treatment ($\bar{x}$ ± SD mass loss = 4.50% ± 11.07%; Kruskal-Wallis χ^2 = 6.7158, p =
311 0.0095) (Figure 5A); however, no significant effects of depth, temperature, CO_2 treatment, or
312 their interactions on peat soil mass loss were observed (Figure 6A; Table S1). Peat C and N
313 content decreased significantly over the course of the experiment (Figure S7), and C:N of the
314 peat was significantly higher at T_f compared to T_0 (Kruskal-Wallis χ^2 = 7.0841, p = 0.0078)
315 (Figure 5B), indicating a more rapid loss of N compared to C. Similar to soil mass loss, neither
316 depth nor the treatment variables had a significant effect on the change in C:N (Figure 6B; Table
317 S1).

318 Results of Fourier-transform infrared spectroscopy (FTIR) analyses further showed limited
319 effects of the treatments on peat soil composition after three years of incubation. Aromatics (%)
320 decreased significantly over the course of the experiment (Figure 5C), but there was no
321 significant effect of soil depth or treatment on the change in aromatics (Figure 6C; Table S1).
322 Depth significantly impacted the change in % carbohydrates, with largest change in the %

323 carbohydrates at 0-10 cm. However, there was no significant difference in % carbohydrates
324 between T_0 and T_f (Figure 5D), and temperature and CO_2 treatment did not significantly impact
325 carbohydrate content (Figure 6D; Table S1).

326 **4. Discussion:**

327 The effects that climate change will have on peatland microbial communities and the
328 resulting impacts on soil decomposition have yet to be fully resolved but could have outsized
329 effects due to the massive stores of carbon in peatlands. Previous results from SPRUCE have
330 shown rapid loss of carbon presumably driven by increased decomposition in response to
331 elevated temperature [10]. In this study, we utilized decomposition ladders to investigate the
332 effects of warming and elevated CO_2 on peat microbial communities and decomposition while
333 limiting inputs from primary productivity. Our results show that bacterial/archaeal and fungal
334 communities are significantly impacted by the SPRUCE treatments; however, in contrast to
335 previous research, we did not observe a significant effect of temperature, elevated CO_2, or soil
336 depth on mass loss or compositional changes. An average of less than 4.5% of the initial mass
337 was lost over the three-year experiment regardless of treatment, demonstrating the high
338 recalcitrance of organic soils in peatlands, and suggesting that these prior reported results may
339 driven by turnover of more recently fixed C rather than the historic C stocks of peat studied here.
340 These small differences also illustrate just how inherently difficult measure such decomposition
341 is to measure given unavoidable experimental variability between replicates and other sources of
342 error, combined with small mass losses of these recalcitrant substrates.

343 Bacterial/archaeal and fungal community compositions were significantly influenced by the
344 SPRUCE treatments (Figure 1, Table 1), indicating that increased temperature and atmospheric
345 CO_2 as a result of climate change may alter microbial ecology in peatlands. Consistent with

346 previous research, bacterial/archaeal community responses to temperature treatment were more
347 pronounced than fungal responses [22, 48, 49]. Bacterial/archaeal α-diversity was significantly
348 highest in the warmest SPRUCE enclosures across all soil depths, whereas the influence of
349 temperature treatment on fungal α-diversity was depth specific and only observed at q=2 (Figure
350 2, Table 2). Ecosystem disturbance and environmental stress have been negatively correlated
351 with microbial diversity [50], thus higher bacterial/archaeal diversity in warmed enclosures
352 suggests that warming may alleviate environmental stress on prokaryotic communities in
353 peatlands. Higher bacterial/archaeal diversity may be a direct cause of warming; however,
354 contrasting results have also been observed in anaerobic peat soil microcosms that investigated
355 direct warming effects [17, 21]. Indirect effects such as warming-induced increases in substrate
356 and nutrient availability [51] are therefore more likely driving changes in bacterial/archaeal
357 diversity by partially relieving nutrient stress. Our experimental design did not allow us to
358 delineate between direct and indirect effects of warming, as porewater total organic carbon and
359 nutrient concentrations were largely correlated with temperature treatment on average over the
360 course of the experiment (Table S2). However, previous research has demonstrated that labile
361 substrate and nutrient availability and microbial diversity are positively correlated which
362 supports our results.

363 Network analyses further revealed the impact of increased temperature on peat microbial
364 community structure. The number of nodes and edges were highest in the networks from warmed
365 enclosures (Figure 3), and a positive correlation between the number of input ASVs and edge
366 and node counts indicates that this is likely a reflection of species richness. Species richness and
367 changes in network topology such as a decreased ratio of positive to negative edges and
368 increased modularity in microbial networks have been shown to correspond to higher community

369 stability [50, 52, 53], potentially through increased microbial functional redundancy [54]. Paired
370 with diversity measures, our network results indicate that warming may positively influence
371 microbial community stability.

372 The abundance of microbial hub taxa (those taxa which are highly connected within the
373 network) was positively correlated with temperature treatment (Figure 3D). The number of hub
374 taxa within microbial networks has been associated with functional potential of the microbial
375 community [55, 56], and hub taxa may exert strong influence over microbiome structure and
376 ecosystem function regardless of their relative abundance within the community [57, 58].
377 Therefore, our results suggest that warming may promote increased microbial functional
378 potential in these peatland ecosystems.

379 We observed *Methanomicrobia*, *Methanobacteria*, and *Methanosarcinia* hubs in the +6.75
380 ºC and +9 ºC networks (Figure 4), supporting results that show methanogenesis is an
381 increasingly important function in peatland carbon-cycle response to warming. The relative
382 abundance of methanogenic taxa has been shown to increase in response to increasing
383 temperature in incubations [17], and rates of methane production have largely been shown to
384 increase with warming [59], including in incubation studies of soil from the S1 bog [17].
385 Detection of an acetoclastic methanogen in the +9 ºC network corresponds to isotopic analysis of
386 CH_4 in the SPRUCE enclosures indicating that acetoclastic methanogenesis is increasing with
387 warming [59]. A significant linear relationship between *in situ* porewater concentrations of CH_4
388 and temperature treatment has been observed in the top 25 cm of soil at SPRUCE [12], further
389 supporting our results. Methane has a global warming potential of 28 times that of CO_2 on a 100-
390 year time span [6], and higher potential for methanogenesis in response to climate change may
391 fuel a positive feedback loop.

392 Methanogenesis can be supported by syntrophic interactions, especially under nutrient-
393 limiting conditions that are observed in bogs [60, 61]. Two known syntrophic taxa, *Syntrophia*
394 [62] and *Syntrophorhabdia* [63], were identified as hubs within the networks (Figure 4),
395 suggesting the potential importance of syntrophy within the sites. Other hubs identified in the
396 networks from warmed enclosures including *Bathyarchaeia* and *Holophagae* may further
397 support increased acetoclastic methanogenesis, as these taxa have been previously shown to have
398 the potential for acetogenesis in anoxic environments [64, 65].
399 Studies of peatland responses to disturbance often investigate fungal and bacterial/archaeal
400 communities independent of one-another despite knowledge of the complex interplay across
401 microbial domains [66, 67]. Here, we observed the highest number of fungal nodes and hub taxa
402 in networks from decomposition ladders in warmed enclosures, suggesting that peatland
403 warming may promote trans-domain interactions, further arguing for such holistic approaches.
404 Possible saprotrophic and ectomycorrhizal fungal hub taxa were primarily observed in the
405 networks from warmed enclosures apart from an *Agaricomycetes* hub in the +0 ºC network
406 (Figure 4). Fungal communities play an important role in organic-matter (OM) decomposition in
407 peatlands [68], and warming may favor dominance of saprotrophic and mycorrhizal fungi from
408 *Basidiomycota* and *Ascomycota* [69], as partially observed in our study. Additionally, warming
409 treatments in these systems are inextricably linked to drying of the peat surface and increased
410 depths to water table. It is thus possible that peat drying and water table changes, more so than
411 warming, may be responsible for the shifts in fungal communities observed; however, the
412 average water table height was similar across all SPRUCE enclosures in the week prior to
413 termination of the experiment (0.17 m ± 2.47 cm) as well as the three prior months.

In contrast to bacterial/archaeal diversity, fungal α-diversity was significantly lower under elevated CO_2 compared to ambient. Fungal responses to CO_2 treatment are likely mediated by plant responses, as CO_2 treatment at SPRUCE is above-ground and is unlikely to directly alter soil biogeochemistry. Interactions between plant roots and fungi are common, and fungi are most prevalent (absolute abundance) near the surface of the peatland where active plant growth occurs [70]. Our results are intriguing and suggest further investigation into plant-fungal interactions under elevated CO_2 conditions.

Significant changes in the peat microbial communities in response to SPRUCE treatments were not mirrored by the peat soil decomposition rates. We anticipated that increased temperature would result in increased peat soil mass loss, as temperature treatment at SPRUCE has resulted in rapid carbon loss that was presumed to be driven by enhanced decomposition [10], increased CO_2 and CH_4 in porewaters [12], and increased microbial respiration of solid phase peat [13]. However, our results showed that soil mass loss and C:N were not significantly impacted by temperature or CO_2 treatment over the course of three years (Figure 6). The lack of differences is likely driven by the short time scale and low initial mass of peat soil in the decomposition bag study compared to the SPRUCE enclosures. Hanson et al. (2020) estimated the rate of carbon loss from SPRUCE to be 31.3 g $C \cdot m^{-2} \cdot year^{-1} \cdot {}^{o}C^{-1}$using approaches including elevation changes and ecosystem CO_2 flux mass balances. Using this rate to estimate the expected loss of carbon from the peat decomposition ladders suggests that differences in mass loss across temperature treatments were on the order of milligrams over a three-year period, thus likely requiring a level of precision that we were unable to be obtain in our litter bag-based experiments.

On average, only 4.5% of the initial peat soil mass was lost over the course of the experiment (Figure 5). The low mass loss demonstrated the recalcitrance of the organic soils in the decomposition ladders is likely driven by a combination of factors including the anoxic, acidic, and oligotrophic conditions of the sites, as well as the chemical composition of the peat. Peat soils at SPRUCE are largely derived from *Sphagnum*, which is known to engineer acidic, nutrient poor, waterlogged conditions [71, 72] and produces anti-microbial compounds and metabolites [73, 74], thereby inhibiting microbial degradation processes. Even the mass loss of fresh *Sphagnum* litter in decomposition bags has been previously shown to be similarly low with only ~10% of initial mass lost after two years [75, 76], so these lower rates for peat soil should not be unexpected.

Diffusion of exogenous dissolved organic matter (DOM) into the decomposition ladders may have also help explain the differences in results between mass loss and community change. Dissolved organic matter is preferentially mineralized by peatland microorganisms when compared to solid-phase peat [77], and fresh plant inputs of DOM can even fuel microbial respiration in deep peat soils [78]. Utilization of exogenous DOM may also partially explain discrepancies between our results and previous results from SPRUCE that have shown increased CO_2 and CH_4 production with warming. Porewater concentrations of total organic carbon were highest in the + 9 ºC enclosures near the termination of our experiment, and higher inputs of DOM may have led to increased OM mineralization and shifts in microbial community structure without impacting peat soil mass in the decomposition ladders.

Similar to soil mass-loss observations, FTIR analysis indicated that temperature and CO_2 treatment had no effect on changes in peat soil composition. The relatively short duration of the experiment may have masked temperature effects on the percent aromatics and carbohydrates of

the peat, although previous results have indicated that carbon at SPRUCE is compositionally stable [79]. We are hopeful that our future planned ladder extractions at our site with their longer field incubation periods may allow for better assessment of treatment effects on peat soil decomposition.

Conclusions

While we did not observe changes in peat soil mass or composition across the SPRUCE treatments in this study, much previous research from the SPRUCE experiment has shown loss of OM near the surface and increased greenhouse gas production in response to elevated temperatures. Our results suggest that these losses in OM may be driven by changes in microbial community structure and dynamics, as we observed significant changes in microbial diversity and network structure in response to warming. The apparent decoupling of changes in peat soil mass and composition and microbial communities may be limited by the very slow peat decomposition rates and precision of mass loss estimates in our study. Collectively, our results and previous results from the SPRUCE experiment therefore suggest that climate change may alter peatland microbial ecology however the ultimate effects of these changes in on rates of degradation of OM and greenhouse gas production in boreal regions remains unclear at this time.

Acknowledgements

We would like to thank Randy Hedin and Evelyn Magner (US Forest Service Northern Research Station) for their assistance in assembling and testing the peat decomposition ladders. This research was sponsored by the Environmental Systems Science Program, U.S. Department of Energy, Office of Science, Biological, and Environmental Research, as part of the Terrestrial Ecosystem Science Scientific Focus Area at Oak Ridge National Laboratory. Oak Ridge National Laboratory is managed by UT-Battelle, LLC, for the U. S. Department of Energy under

contract DE-AC05-00OR22725. This research used resources of the Compute and Data Environment for Science (CADES) at the Oak Ridge National Laboratory, which is supported by the Office of Science of the U.S. Department of Energy under Contract No. DE-AC05-00OR22725.

Author contribution statement

Conceptualization – NAG, PJH, RKK, CWS; Investigation – SR, RKK, NAG, KCO, AAC, AS, JPC, DMK; Formal analysis – SR; Original draft writing – SR; Draft revision – SR, RKK, NAG, KCO, AAC, AS, JPC, DMK, CWS

ORCID:

SR: 0000-0001-9559-1154

NAG: 0000-0003-0068-7714

RKK: 0000-0002-6419-8218

PJH: 0000-0001-7293-3561

KCO: 0000-0002-0875-2720

AAC: 0000-0003-1142-4709

DMK: 0000-0002-4307-2560

AS: 0000-0001-8269-9270

JPC: 0000-0002-3303-9708

CWS: 0000-0001-8759-2448

Table 1: Results of permutational multivariate analysis of variance (PERMANOVA) of bacterial/archaeal and fungal community compositions based on Bray-Curtis distances. Significant factors and interactive effects ($p < 0.05$) are bolded.

Variable	Bacterial/Archaeal			Fungal		
	F-Statistic	R^2	p-value	F-Statistic	R^2	p-value
Depth	15.402	0.25323	**0.001**	4.0315	0.10959	**0.001**
Temperature Treatment	11.1683	0.06121	**0.001**	5.46	0.04948	**0.001**
CO_2 Treatment	3.3775	0.01851	**0.004**	3.0053	0.02723	**0.001**
Depth:Temperature Treatment	2.907	0.03766	**0.001**	1.9049	0.05178	**0.001**
Depth:CO_2 Treatment	1.2092	0.01988	0.176	1.6339	0.04442	**0.006**
Temperature treatment:CO_2 treatment	4.983	0.02731	**0.001**	2.6901	0.02438	**0.004**
Depth:Temperature Treatment:CO_2 Treatment	1.4101	0.02318	0.069	1.8305	0.04976	**0.001**

Table 2: Resulting p-values from ANOVA describing the effects of depth and SPRUCE treatments on bacterial/archaeal and fungal α-diversity across Hill numbers (q=0, q=1, and q=2). Significant values ($p < 0.05$) are bolded.

Variable	16S			ITS		
	q=0	**q=1**	**q=2**	**q=0**	**q=1**	**q=2**
Depth	**<0.001**	**<0.001**	**<0.001**	**<0.001**	0.802	0.296
Temperature Treatment	**0.002**	**<0.001**	**<0.001**	0.728	0.113	**0.034**
CO_2 Treatment	**<0.001**	**0.015**	0.133	**0.009**	**<0.001**	**0.002**
Depth:Temperature Treatment	0.978	0.907	0.856	0.094	**0.013**	**0.003**

Figure Captions:

Figure 1: Principal coordinates analysis of Bray-Curtis dissimilarities of bacterial/archaeal (A) and fungal (B) communities in decomposition ladders. Points are colored based on sample depth, filled based on enclosure CO_2 treatments and shaped based on enclosure temperature treatments.

Figure 2: Bacterial/Archaeal (A) and Fungal (B) α-diversity at q = 0 (species richness) across depths (vertical facets/colors), CO_2 treatments (horizontal facets), and temperature treatments (x-axis).

Figure 3: Summary of network topologies for temperature treatment microbial networks. The number of edges (A) represents the sum total connections between taxa (nodes; B) within the network. Mean degree (C) represents the average number of connections per taxon. Hubs (D) are defined as nodes within the network that are in the 90th percentile for degree and betweenness centrality and represent highly connected and centralized taxa.

Figure 4: Class-level distribution of network hubs across temperature treatments (color). Hubs were aggregated at class-level taxonomic annotations (y-axis) and faceted by kingdom-level taxonomy.

Figure 5: Comparisons of peat soil oven dry mass (A), carbon:nitrogen (B), percent aromatics (C), and percent carbohydrates (D) in peat decomposition ladders at the start of the experiment (T_0) and after three years of incubation in the SPRUCE enclosures (T_f). Box and whisker plots display the median (middle of box), quartiles (top and bottom of box), minimum and maximum values excluding outliers (end of whisker) and outliers (points).

Figure 6: Peat mass loss (% of starting mass lost) (A), percent C:N change ($T_f - T_0$) (B), percent aromatics change ($T_f - T_0$) (C), and percent carbohydrates change ($T_f - T_0$) (D) across depths (facets) and temperature treatments (x-axis).

References:

1. Turunen, J., et al., *Estimating carbon accumulation rates of undrained mires in Finland - application to boreal and subarctic regions.* Holocene, 2002. **12**(1): p. 69-80.
2. Nichols, J.E. and D.M. Peteet, *Rapid expansion of northern peatlands and doubled estimate of carbon storage.* Nature Geoscience, 2019. **12**(11): p. 917-+.
3. Vitt, D.H., et al., *Spatial and temporal trends in carbon storage of peatlands of continental western Canada through the Holocene.* Canadian Journal of Earth Sciences, 2000. **37**(5): p. 683-693.
4. Andersen, R., S.J. Chapman, and R.R.E. Artz, *Microbial communities in natural and disturbed peatlands: A review.* Soil Biology & Biochemistry, 2013. **57**: p. 979-994.
5. Bridgham, S.D., et al., *Methane emissions from wetlands: biogeochemical, microbial, and modeling perspectives from local to global scales.* Global Change Biology, 2013. **19**(5): p. 1325-1346.
6. IPCC, *Climate Change 2013: The Physical Science Basis. Contribution of Working Group I to the Fifth Assessment Report of the Intergovernmental Panel on Climate Change*. 2013, Cambridge, United Kingdom and New York, NY, USA: Cambridge University Press. 1535.
7. Crowther, T.W., et al., *Quantifying global soil carbon losses in response to warming.* Nature, 2016. **540**(7631): p. 104-+.
8. Davidson, E.A. and I.A. Janssens, *Temperature sensitivity of soil carbon decomposition and feedbacks to climate change.* Nature, 2006. **440**(7081): p. 165-173.
9. Bridgham, S.D., et al., *The carbon balance of North American wetlands.* Wetlands, 2006. **26**(4): p. 889-916.
10. Hanson, P.J., et al., *Rapid Net Carbon Loss From a Whole-Ecosystem Warmed Peatland.* Agu Advances, 2020. **1**(3).
11. Norby, R.J., et al., *Rapid loss of an ecosystem engineer: Sphagnum decline in an experimentally warmed bog.* Ecology and Evolution, 2019. **9**(22): p. 12571-12585.
12. Wilson, R.M., et al., *Soil metabolome response to whole-ecosystem warming at the Spruce and Peatland Responses under Changing Environments experiment.* Proceedings of the National Academy of Sciences of the United States of America, 2021. **118**(25).
13. Wilson, R.M., et al., *Radiocarbon Analyses Quantify Peat Carbon Losses With Increasing Temperature in a Whole Ecosystem Warming Experiment.* Journal of Geophysical Research-Biogeosciences, 2021. **126**(11).
14. Schadel, C., et al., *Potential carbon emissions dominated by carbon dioxide from thawed permafrost soils.* Nature Climate Change, 2016. **6**(10): p. 950-+.
15. Tveit, A.T., et al., *Metabolic and trophic interactions modulate methane production by Arctic peat microbiota in response to warming.* Proceedings of the National Academy of Sciences of the United States of America, 2015. **112**(19): p. E2507-E2516.
16. Yvon-Durocher, G., et al., *Methane fluxes show consistent temperature dependence across microbial to ecosystem scales.* Nature, 2014. **507**(7493): p. 488-491.
17. Kolton, M., et al., *Impact of Warming on Greenhouse Gas Production and Microbial Diversity in Anoxic Peat From a Sphagnum-Dominated Bog (Grand Rapids, Minnesota, United States).* Frontiers in Microbiology, 2019. **10**.
18. Kluber, L.A., et al., *Constraints on microbial communities, decomposition and methane production in deep peat deposits.* Plos One, 2020. **15**(2).

19. Keiser, A.D., et al., *Peatland microbial community response to altered climate tempered by nutrient availability.* Soil Biology & Biochemistry, 2019. **137**.
20. AminiTabrizi, R., et al., *Elevated temperatures drive abiotic and biotic degradation of organic matter in a peat bog under oxic conditions.* Science of the Total Environment, 2022. **804**.
21. Yang, S.Z., et al., *Decoupling of microbial community dynamics and functions in Arctic peat soil exposed to short term warming.* Molecular Ecology, 2021. **30**(20): p. 5094-5104.
22. Lulakova, P., et al., *High-Alpine Permafrost and Active-Layer Soil Microbiomes Differ in Their Response to Elevated Temperatures.* Frontiers in Microbiology, 2019. **10**.
23. Hopple, A.M., et al., *Massive peatland carbon banks vulnerable to rising temperatures.* Nature Communications, 2020. **11**(1).
24. Wilson, R.M., et al., *Stability of peatland carbon to rising temperatures.* Nature Communications, 2016. **7**.
25. Wilson, R.M., et al., *Functional capacities of microbial communities to carry out large scale geochemical processes are maintained during ex situ anaerobic incubation.* Plos One, 2021. **16**(2).
26. Krishna, M.P. and M. Mohan, *Litter decomposition in forest ecosystems: a review.* Energy, Ecology and Environment, 2017. **2**: p. 236-249.
27. Tfaily, M.M., et al., *Vertical Stratification of Peat Pore Water Dissolved Organic Matter Composition in a Peat Bog in Northern Minnesota.* Journal of Geophysical Research-Biogeosciences, 2018. **123**(2): p. 479-494.
28. Hanson, P.J., et al., *Attaining whole-ecosystem warming using air and deep-soil heating methods with an elevated CO2 atmosphere.* Biogeosciences, 2017. **14**(4): p. 861-883.
29. Weiss, J.V., D. Emerson, and J.P. Megonigal, *Rhizosphere iron(III) deposition and reduction in a Juncus effusus L.-dominated wetland.* Soil Science Society of America Journal, 2005. **69**(6): p. 1861-1870.
30. Kirwan, M.L., et al., *The impact of sea-level rise on organic matter decay rates in Chesapeake Bay brackish tidal marshes.* Biogeosciences, 2013. **10**(3): p. 1869-1876.
31. Hodgkins, S.B., et al., *Tropical peatland carbon storage linked to global latitudinal trends in peat recalcitrance.* Nature Communications, 2018. **9**.
32. Dove, N.C., et al., *Microbiome Variation Across Two Hemlock Species With Hemlock Woolly Adelgid Infestation.* Frontiers in Microbiology, 2020. **11**.
33. Rogers, T.J., et al., *Exploring variation in phyllosphere microbial communities across four hemlock species.* Ecosphere, 2018. **9**(12).
34. Bolyen, E., et al., *Reproducible, interactive, scalable and extensible microbiome data science using QIIME 2.* Nature Biotechnology, 2019. **37**(8): p. 852-857.
35. Martin, M., *Cutadapt removes adapter sequences from high-throughput sequencing reads.* 2011, 2011. **17**(1): p. 3.
36. Callahan, B.J., et al., *DADA2: High-resolution sample inference from Illumina amplicon data.* Nature Methods, 2016. **13**(7): p. 581-+.
37. Quast, C., et al., *The SILVA ribosomal RNA gene database project: improved data processing and web-based tools.* Nucleic Acids Research, 2013. **41**(D1): p. D590-D596.
38. Nilsson, R.H., et al., *The UNITE database for molecular identification of fungi: handling dark taxa and parallel taxonomic classifications.* Nucleic Acids Research, 2019. **47**(D1): p. D259-D264.

39. Price, M.N., P.S. Dehal, and A.P. Arkin, *FastTree 2-Approximately Maximum-Likelihood Trees for Large Alignments.* Plos One, 2010. **5**(3).
40. Oksanen, J., et al., *vegan: Community Ecology Package*. 2020.
41. McMurdie, P.J. and S. Holmes, *phyloseq: An R Package for Reproducible Interactive Analysis and Graphics of Microbiome Census Data.* Plos One, 2013. **8**(4).
42. Villanueva, R.A.M. and Z.J. Chen, *ggplot2: Elegant Graphics for Data Analysis, 2nd edition.* Measurement-Interdisciplinary Research and Perspectives, 2019. **17**(3): p. 160-167.
43. Kurtz, Z.D., et al., *Sparse and Compositionally Robust Inference of Microbial Ecological Networks.* Plos Computational Biology, 2015. **11**(5).
44. Csardi, G. and T. Nepusz, *The igraph software package for complex network research.* InterJournal, 2006. **Complex Systems**: p. 1695.
45. Alberdi, A. and M.T.P. Gilbert, *hilldiv: an R package for the integral analysis of diversity based on Hill numbers.* bioRxiv, 2019: p. 545665.
46. Chao, A.N., C.H. Chiu, and L. Jost, *Unifying Species Diversity, Phylogenetic Diversity, Functional Diversity, and Related Similarity and Differentiation Measures Through Hill Numbers.* Annual Review of Ecology, Evolution, and Systematics, Vol 45, 2014. **45**: p. 297-324.
47. Bray, J.R. and J.T. Curtis, *An Ordination of the Upland Forest Communities of Southern Wisconsin.* Ecological Monographs, 1957. **27**(4): p. 326-349.
48. Xiong, J.B., et al., *Divergent Responses of Soil Fungi Functional Groups to Short-term Warming (vol 68, pg 708, 2014).* Microbial Ecology, 2014. **68**(4): p. 890-890.
49. Zhao, B.Y., P. Xing, and Q.L.L. Wu, *Interactions between bacteria and fungi in macrophyte leaf litter decomposition.* Environmental Microbiology, 2021. **23**(2): p. 1130-1144.
50. Hernandez, D.J., et al., *Environmental stress destabilizes microbial networks.* Isme Journal, 2021. **15**(6): p. 1722-1734.
51. Iversen, C.M., et al., *Whole-Ecosystem Warming Increases Plant-Available Nitrogen and Phosphorus in an Ombrotrophic Bog.* Ecosystems, 2022.
52. Thebault, E. and C. Fontaine, *Stability of Ecological Communities and the Architecture of Mutualistic and Trophic Networks.* Science, 2010. **329**(5993): p. 853-856.
53. Tardy, V., et al., *Stability of soil microbial structure and activity depends on microbial diversity.* Environmental Microbiology Reports, 2014. **6**(2): p. 173-183.
54. Griffiths, B.S. and L. Philippot, *Insights into the resistance and resilience of the soil microbial community.* Fems Microbiology Reviews, 2013. **37**(2): p. 112-129.
55. Faust, K., et al., *Cross-biome comparison of microbial association networks.* Frontiers in Microbiology, 2015. **6**.
56. Shi, Y., et al., *Abundance of kinless hubs within soil microbial networks are associated with high functional potential in agricultural ecosystems.* Environment International, 2020. **142**.
57. Banerjee, S., K. Schlaeppi, and M.G.A. van der Heijden, *Keystone taxa as drivers of microbiome structure and functioning.* Nature Reviews Microbiology, 2018. **16**(9): p. 567-576.
58. Xun, W.B., et al., *Specialized metabolic functions of keystone taxa sustain soil microbiome stability.* Microbiome, 2021. **9**(1).

59. Gill, A.L., et al., *Deep peat warming increases surface methane and carbon dioxide emissions in a black spruce-dominated ombrotrophic bog.* Global Change Biology, 2017. **23**(12): p. 5398-5411.
60. McInerney, M.J., J.R. Sieber, and R.P. Gunsalus, *Syntrophy in anaerobic global carbon cycles.* Current Opinion in Biotechnology, 2009. **20**(6): p. 623-632.
61. Morris, B.E., et al., *Microbial syntrophy: interaction for the common good.* Fems Microbiology Reviews, 2013. **37**(3): p. 384-406.
62. McInerney, M.J., et al., *Physiology, ecology, phylogeny, and genomics of microorganisms capable of syntrophic metabolism.* Incredible Anaerobes: From Physiology to Genomics to Fuels, 2008. **1125**: p. 58-72.
63. Qiu, Y.L., et al., *Syntrophorhabdus aromaticivorans gen. nov., sp. nov., the first cultured anaerobe capable of degrading phenol to acetate in obligate syntrophic associations with a hydrogenotrophic methanogen.* Applied and Environmental Microbiology, 2008. **74**(7): p. 2051-2058.
64. He, Y., et al., *Genomic and enzymatic evidence for acetogenesis among multiple lineages of the archaeal phylum Bathyarchaeota widespread in marine sediments.* Nature Microbiology, 2016. **1**(6).
65. Liesack, W., et al., *Holophaga Foetida Gen-Nov, Sp-Nov, a New, Homoacetogenic Bacterium Degrading Methoxylated Aromatic-Compounds.* Archives of Microbiology, 1994. **162**(1-2): p. 85-90.
66. de Vries, F.T., et al., *Soil food web properties explain ecosystem services across European land use systems.* Proceedings of the National Academy of Sciences of the United States of America, 2013. **110**(35): p. 14296-14301.
67. Faust, K. and J. Raes, *Microbial interactions: from networks to models.* Nature Reviews Microbiology, 2012. **10**(8): p. 538-550.
68. Thormann, M.N., *The Role of Fungi in Boreal Peatlands*, in *Boreal Peatland Ecosystems*, R.K. Wieder and D.H. Vitt, Editors. 2006, Springer Berlin Heidelberg: Berlin, Heidelberg. p. 101-123.
69. Asemaninejad, A., et al., *Climate change favours specific fungal communities in boreal peatlands.* Soil Biology & Biochemistry, 2018. **120**: p. 28-36.
70. Lin, X.J., et al., *Microbial Community Stratification Linked to Utilization of Carbohydrates and Phosphorus Limitation in a Boreal Peatland at Marcell Experimental Forest, Minnesota, USA.* Applied and Environmental Microbiology, 2014. **80**(11): p. 3518-3530.
71. Vanbreemen, N., *How Sphagnum Bogs down Other Plants.* Trends in Ecology & Evolution, 1995. **10**(7): p. 270-275.
72. Verhoeven, J.T.A. and W.M. Liefveld, *The ecological significance of organochemical compounds in Sphagnum.* Acta Botanica Neerlandica, 1997. **46**(2): p. 117-130.
73. Fudyma, J.D., et al., *Untargeted metabolomic profiling of Sphagnum fallax reveals novel antimicrobial metabolites.* Plant Direct, 2019. **3**(11).
74. Hajek, T., et al., *Cell-wall polysaccharides play an important role in decay resistance of Sphagnum and actively depressed decomposition in vitro.* Biogeochemistry, 2011. **103**(1-3): p. 45-57.
75. Scheffer, R.A., R.S.P. van Logtestijn, and J.T.A. Verhoeven, *Decomposition of Carex and Sphagnum litter in two mesotrophic fens differing in dominant plant species.* Oikos, 2001. **92**(1): p. 44-54.

76. Verhoeven, J.T.A. and E. Toth, *Decomposition of Carex and Sphagnum Litter in Fens - Effect of Litter Quality and Inhibition by Living Tissue-Homogenates.* Soil Biology & Biochemistry, 1995. **27**(3): p. 271-275.
77. Hopple, A.M., et al., *Does dissolved organic matter or solid peat fuel anaerobic respiration in peatlands?* Geoderma, 2019. **349**: p. 79-87.
78. Tfaily, M.M., et al., *Organic matter transformation in the peat column at Marcell Experimental Forest: Humification and vertical stratification.* Journal of Geophysical Research-Biogeosciences, 2014. **119**(4): p. 661-675.
79. Baysinger, M.R., et al., *Compositional stability of peat in ecosystem-scale warming mesocosms.* Plos One, 2022. **17**(3).

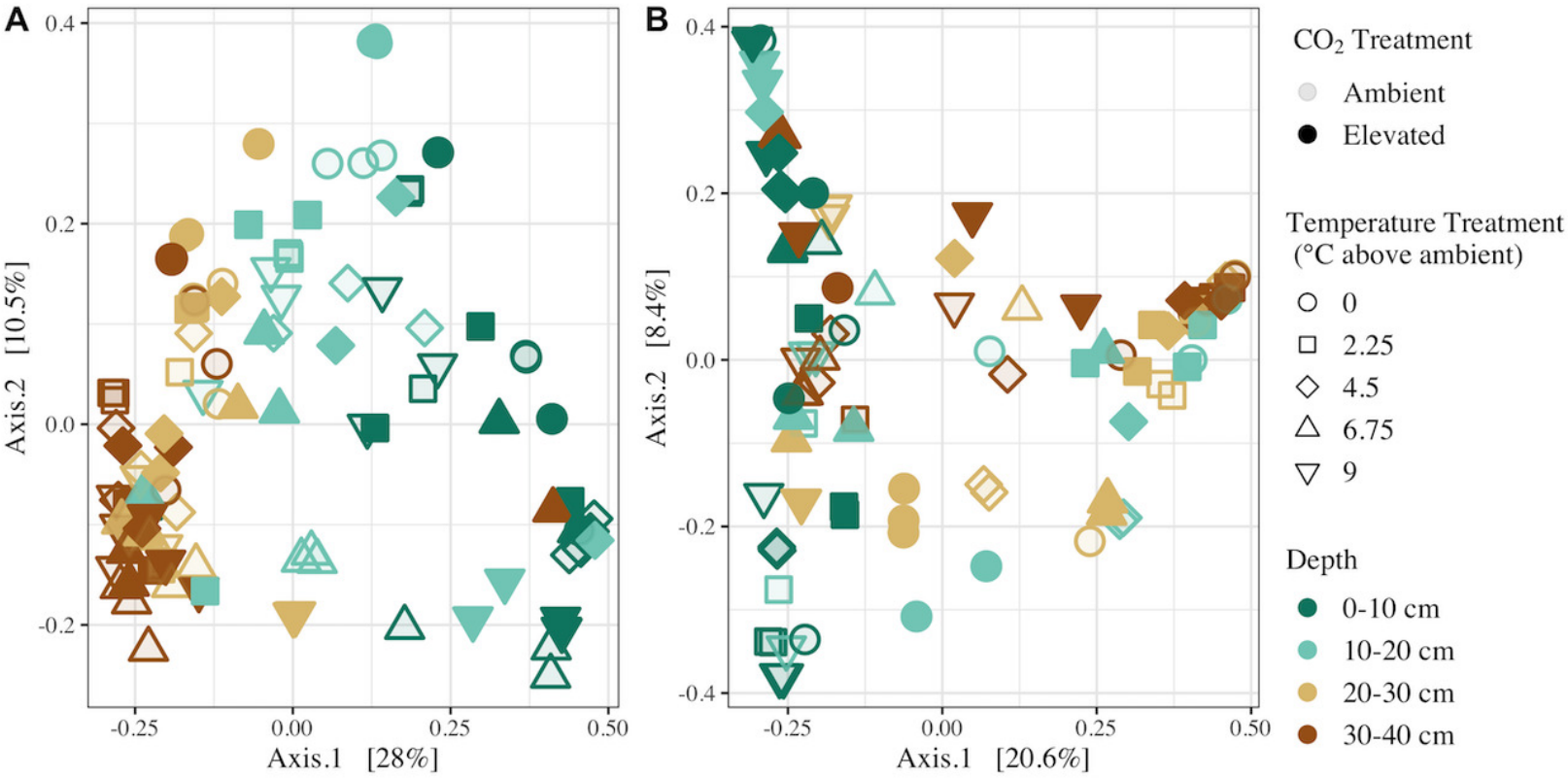
A
B
0.4
0.2
0.0
-0.2
-0.4
-0.25
0.00
0.25
0.50
Axis.1 [28%]
Axis.2 [10.5%]
Axis.1 [20.6%]
Axis.2 [8.4%]
CO2 Treatment
Ambient
Elevated
Temperature Treatment
(°C above ambient)
0
2.25
4.5
6.75
9
Depth
0-10 cm
10-20 cm
20-30 cm
30-40 cm

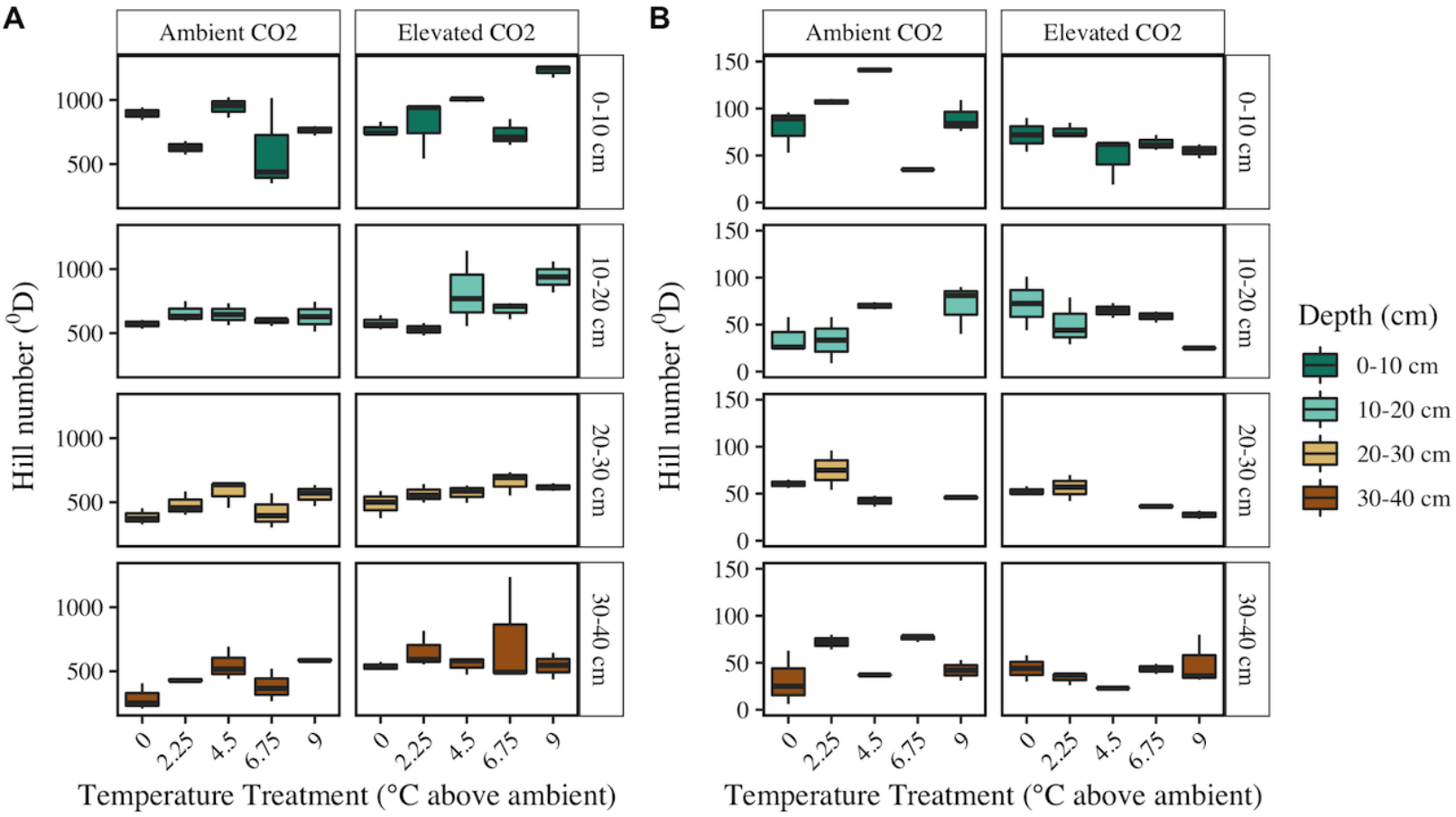
A
B
Ambient CO2
Elevated CO2
0-10 cm
10-20 cm
20-30 cm
30-40 cm
Hill number (⁰D)
Temperature Treatment (°C above ambient)
0
2.25
4.5
6.75
9
Depth (cm)

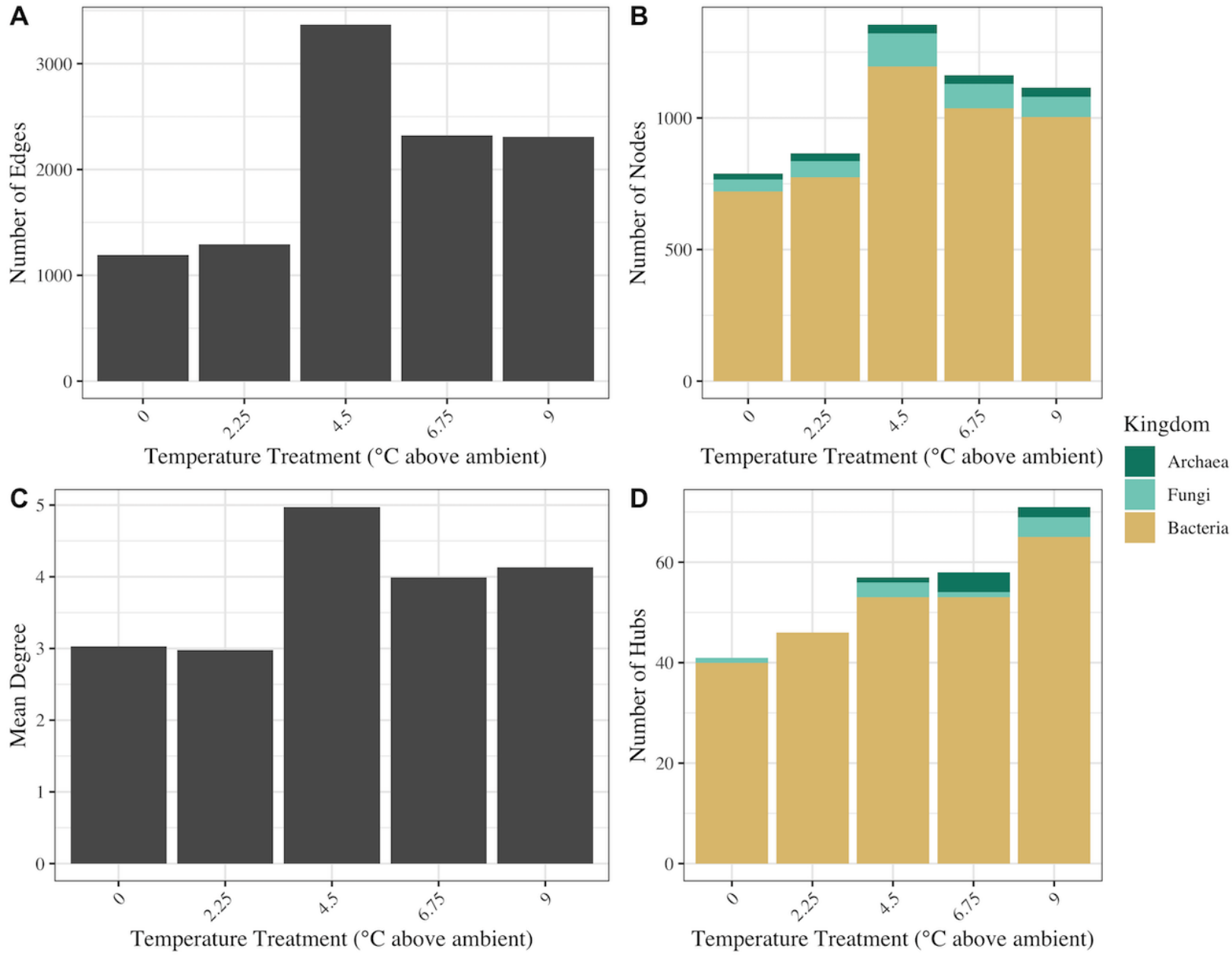
A
Number of Edges
3000
2000
1000
0
0
2.25
4.5
6.75
9
Temperature Treatment (°C above ambient)
B
Number of Nodes
1000
500
0
0
2.25
4.5
6.75
9
Temperature Treatment (°C above ambient)
Kingdom
Archaea
Fungi
Bacteria
C
Mean Degree
5
4
3
2
1
0
0
2.25
4.5
6.75
9
Temperature Treatment (°C above ambient)
D
Number of Hubs
60
40
20
0
0
2.25
4.5
6.75
9
Temperature Treatment (°C above ambient)

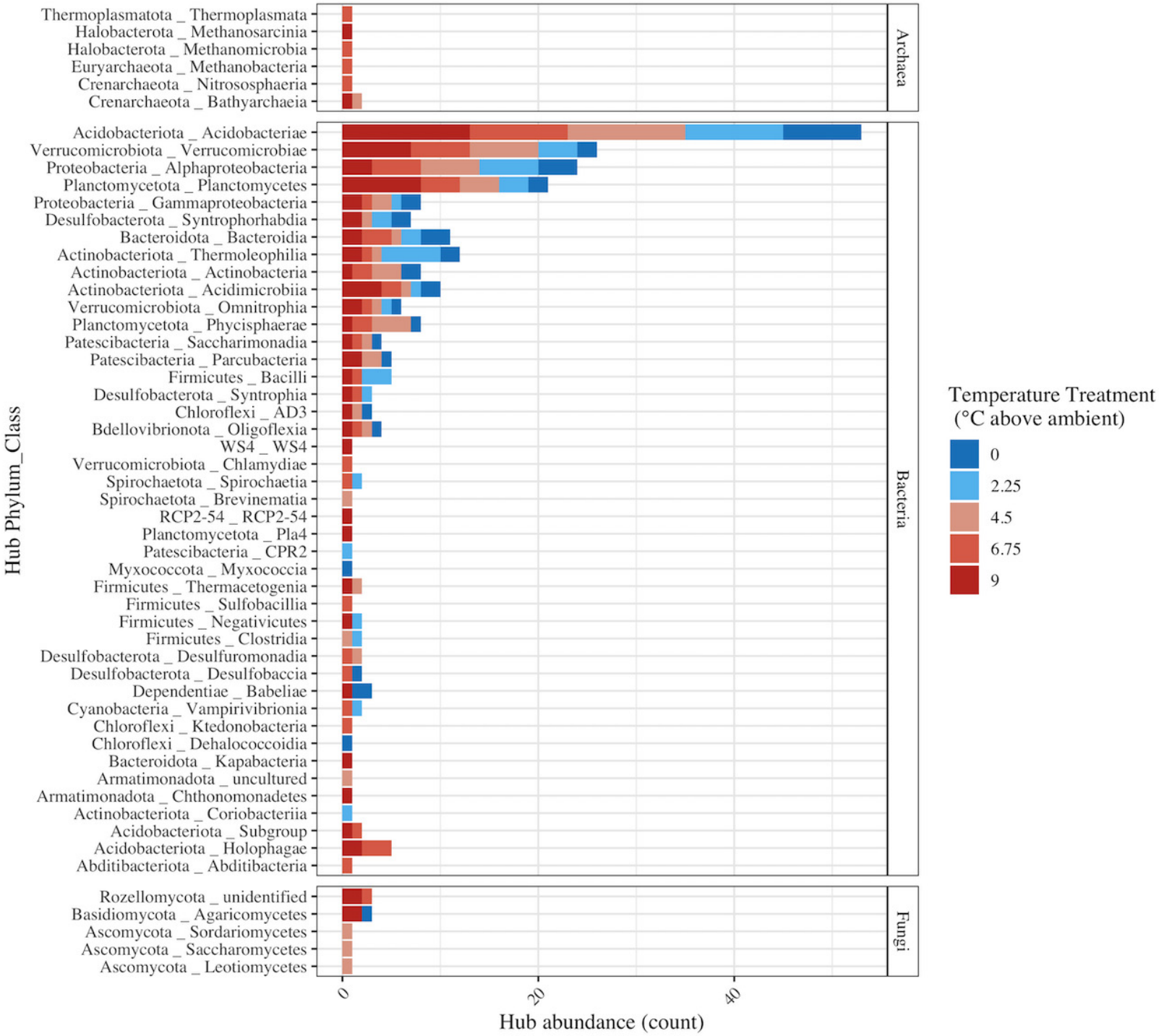
Thermoplasmatota _ Thermoplasmata
Halobacterota _ Methanosarcinia
Halobacterota _ Methanomicrobia
Euryarchaeota _ Methanobacteria
Crenarchaeota _ Nitrososphaeria
Crenarchaeota _ Bathyarchaeia
Archaea
Acidobacteriota _ Acidobacteriae
Verrucomicrobiota _ Verrucomicrobiae
Proteobacteria _ Alphaproteobacteria
Planctomycetota _ Planctomycetes
Proteobacteria _ Gammaproteobacteria
Desulfobacterota _ Syntrophorhabdia
Bacteroidota _ Bacteroidia
Actinobacteriota _ Thermoleophilia
Actinobacteriota _ Actinobacteria
Actinobacteriota _ Acidimicrobiia
Verrucomicrobiota _ Omnitrophia
Planctomycetota _ Phycisphaerae
Patescibacteria _ Saccharimonadia
Patescibacteria _ Parcubacteria
Firmicutes _ Bacilli
Desulfobacterota _ Syntrophia
Chloroflexi _ AD3
Bdellovibrionota _ Oligoflexia
WS4 _ WS4
Verrucomicrobiota _ Chlamydiae
Spirochaetota _ Spirochaetia
Spirochaetota _ Brevinematia
RCP2-54 _ RCP2-54
Planctomycetota _ Pla4
Patescibacteria _ CPR2
Myxococcota _ Myxococcia
Firmicutes _ Thermacetogenia
Firmicutes _ Sulfobacillia
Firmicutes _ Negativicutes
Firmicutes _ Clostridia
Desulfobacterota _ Desulfuromonadia
Desulfobacterota _ Desulfobaccia
Dependentiae _ Babeliae
Cyanobacteria _ Vampirivibrionia
Chloroflexi _ Ktedonobacteria
Chloroflexi _ Dehalococcoidia
Bacteroidota _ Kapabacteria
Armatimonadota _ uncultured
Armatimonadota _ Chthonomonadetes
Actinobacteriota _ Coriobacteriia
Acidobacteriota _ Subgroup
Acidobacteriota _ Holophagae
Abditibacteriota _ Abditibacteria
Bacteria
Rozellomycota _ unidentified
Basidiomycota _ Agaricomycetes
Ascomycota _ Sordariomycetes
Ascomycota _ Saccharomycetes
Ascomycota _ Leotiomycetes
Fungi
Hub Phylum_Class
0
20
40
Hub abundance (count)
Temperature Treatment
(°C above ambient)
0
2.25
4.5
6.75
9

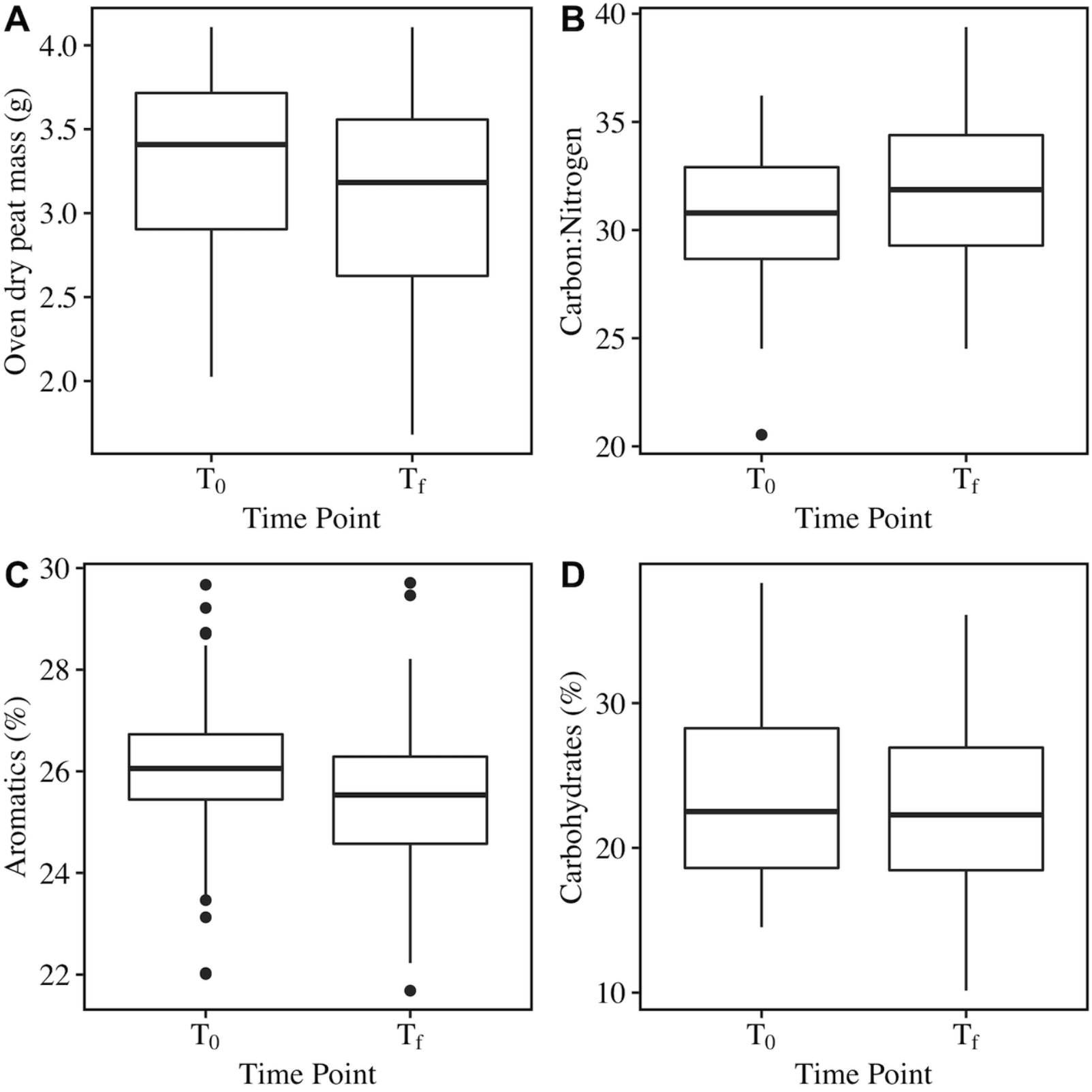
A
Oven dry peat mass (g)
4.0
3.5
3.0
2.5
2.0
T0
Tf
Time Point
B
Carbon:Nitrogen
40
35
30
25
20
T0
Tf
Time Point
C
Aromatics (%)
30
28
26
24
22
T0
Tf
Time Point
D
Carbohydrates (%)
30
20
10
T0
Tf
Time Point

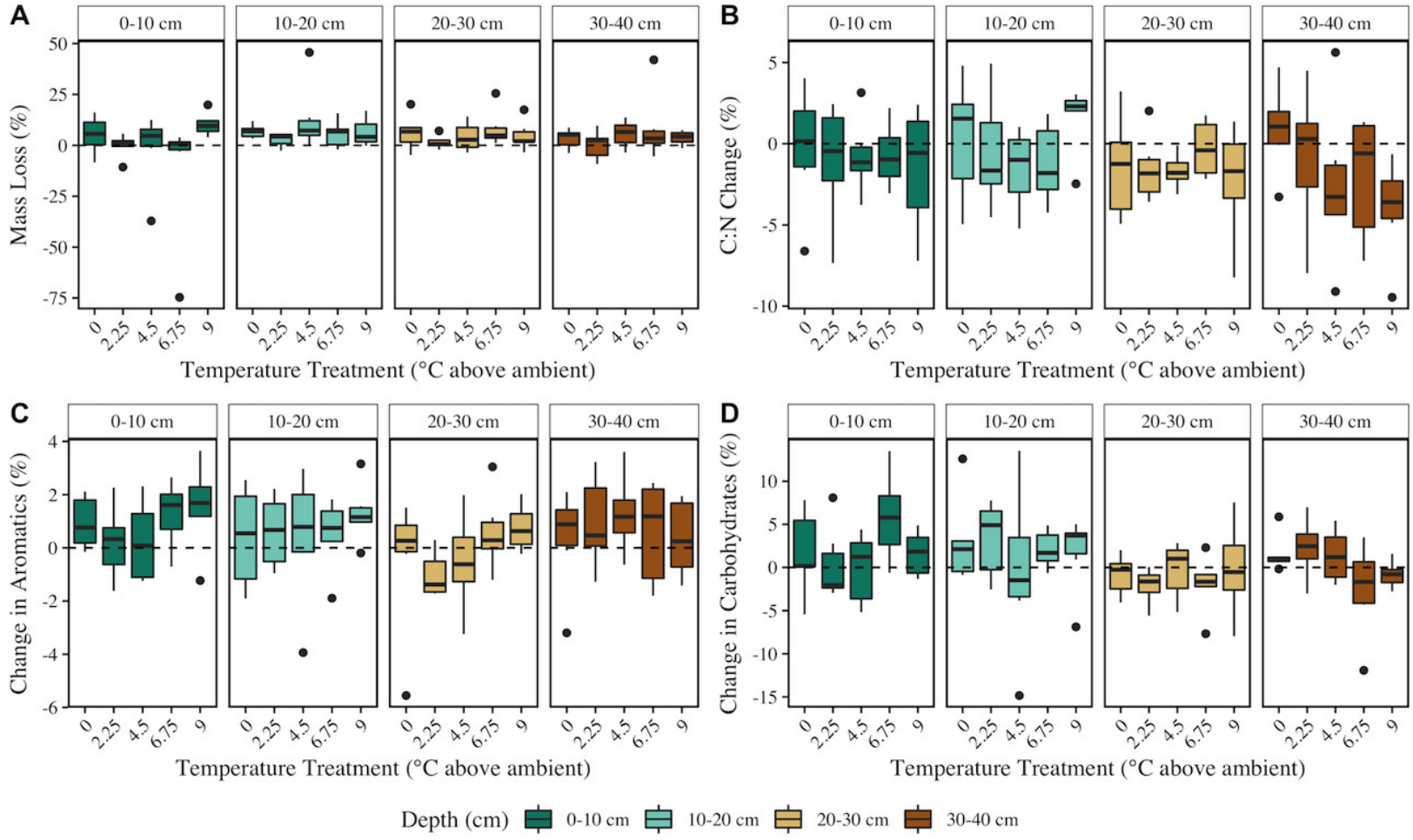
A
0-10 cm
10-20 cm
20-30 cm
30-40 cm
Mass Loss (%)
50
25
0
-25
-50
-75
0
2.25
4.5
6.75
9
Temperature Treatment (°C above ambient)
B
C:N Change (%)
5
0
-5
-10
C
Change in Aromatics (%)
4
2
0
-2
-4
-6
D
Change in Carbohydrates (%)
10
5
0
-5
-10
-15
Depth (cm)
0-10 cm
10-20 cm
20-30 cm
30-40 cm